JPET Fast Forward. Published on March 11, 2011 as DOI: 10.1124/jpet.110.177055
This article has not been copyedited and formatted. The final version may differ from this version.

JPET #177055

Title Page

TREATMENT WITH Z-LIGUSTILIDE, A COMPONENT OF *ANGELICA SINENSIS*, REDUCES BRAIN INJURY FOLLOWING A SUBARACHNOID HEMORRHAGE IN RATS

Di Chen, Jiping Tang, Nikan H. Khatibi, Mei Zhu, Yingbo Li, Chengyuan Wang, Rong Jiang, Liu Tu, Shali Wang

Institute of Neuroscience, Chongqing Medical University, Chongqing, China (D.C., M.Z., Y.L., R.J., L.T., S.W.);

Department of Physiology and Pharmacology, Loma Linda University, Loma Linda, California, USA (J. T.);

Department of Anesthesiology, Loma Linda University, Loma Linda, California, USA (N.H.K.);

Department of Physiology, Luzhou Medical College, Luzhou, Sichuan, China (M. Z.);

Research Center of Medical Chemistry and Chemical Biology, Chongqing Technology and Business University, Chongqing, China (C.Y.)

JPET #177055

Running Title Page

Running title: LIG reduces brain injury following SAH

Corresponding author: Shali Wang

Institute of Neuroscience, Chongqing Medical University, Chongqing, China, 400016

Tel: +86-23-68892728 Fax: +86-23-67084567 E-mail: ypshali2010@gmail.com

Number of text pages: 32

Number of tables: 0

Number of figures: 10

Number of references: 34

Number of words:

Abstract: 250

Introduction: 370

Discussion: 827

Abbreviations: ANOVA, analysis of variance; BA, basilar artery; BBB, Blood-Brain Barrier; CVS, cerebral vasospasm; EB, Evans blue; LIG, Z-ligustilide; PBS, phosphate buffer solution; SAH, subarachnoid hemorrhage; SD, Sprague-Dawley; SNK, Student-Newman-Keuls; TUNEL, TdT-mediated dUTP-biotin nick end labeling

Recommended section: Neuropharmacology

JPET Fast Forward. Published on March 11, 2011 as DOI: 10.1124/jpet.110.177055
This article has not been copyedited and formatted. The final version may differ from this version.

Abstract

Subarachnoid hemorrhage (SAH) is a devastating stroke subtype accounting for 3~7% of cases each year. Despite its rarity among the various stroke types, SAH is still responsible for roughly 25% of all stroke fatalities. Although various preventative and therapeutic interventions have been explored for potential neuroprotection following SAH, a considerable percentage of patients still experience serious neurologic and/or cognitive impairments as a result of the primary hemorrhage and/or secondary brain damage that occurs. Z-Ligustilide (LIG), the primary lipophilic component of the Chinese traditional medicine *Radix Angelica Sinensis*, has been shown to reduce ischemic brain injury via anti-apoptotic pathways. Accordingly, in our study, we investigated the neuroprotective potential of LIG following experimental SAH in rats. Rats with SAH induced using the established double hemorrhage model were administered with or without LIG treatment. Mortality, neurobehavioral evaluation, brain water content, blood brain barrier (BBB) permeability, and vasospasm assessment of the basilar artery were measured on days 3 and 7 after injury. Additional testing was done to evaluate for apoptosis using TUNEL staining as well as immunohistochemistry and western blotting to identify key pro-apoptotic/survival proteins i.e. p53, Bax, Bcl-2 and cleaved caspase-3. The results showed that LIG post-treatment reduced mortality, neurobehavioral deficits, brain edema, BBB permeability, and cerebral vasospasm. Additionally, treatment reduced the number of apoptotic cells in the surrounding brain injury site which accompanied a marked down-regulation of pro-apoptotic proteins, p53 and cleaved caspase-3. Our data suggest that LIG may be an effective therapeutic modality for SAH victims by altering apoptotic mechanisms.

JPET Fast Forward. Published on March 11, 2011 as DOI: 10.1124/jpet.110.177055
This article has not been copyedited and formatted. The final version may differ from this version.

Introduction

Subarachnoid hemorrhage (SAH) is a devastating stroke subtype with a significantly high morbidity and mortality rate (Tseng MY et al., 2005; Janjua N and Mayer SA, 2003). Despite promising therapeutic approaches – surgical treatment, triple-H therapy (Rosenwasser RH et al., 1999), calcium channel blockers, endothelin-receptor antagonists (Vajkoczy P et al., 2005) and sodium nitroprusside therapy (Raabe A et al., 2002) – successful treatment following SAH remains inadequate. This is partly attributed to the lack of effective therapeutic approach in dealing with cerebral ischemia as a result of cerebral vasospasm, one of the major consequences seen following an SAH. As a result, a new therapeutic approach is warranted to combat the effects of cerebral vasospasm and hopefully improve prognosis.

Angelica sinensis, commonly known as the female ginseng, is a well known traditional Chinese medicine used for thousands of years to treat various gynecological diseases (Tsuchida T et al, 1987; Liu J et al, 2001), immune system disorders (Wilasrusmee C et al, 2002), and for prevention of platelet aggregation (Shimizu M et al, 1991) in patients. One of the major components of *Angelica sinensis*, Z-Ligustilide (3-butylidene-4, 5-dihydrophthalide, LIG) (Fig. 1) (Kuang X et al., 2006), has been considered to be the active ingredient responsible for its beneficial effects. Previously published works have alluded to the antioxidant effects induced by a decrease in malondialdehyde and increase activity of glutathione peroxidase and superoxide dismutase as the mechanism behind its protection. Yet alternative published data has directed its attention more to the anti-apoptotic mechanisms of LIG - specifically via up-regulation of Bcl-2 and down-regulation of Bax and caspase-3 (Kuang X et al, 2006). Nonetheless, LIG has been shown to significantly reduce infarction size and brain edema formation as well as improve neurobehavioral deficits caused by focal cerebral ischemia (Peng HY et al, 2007) as well as in transient forebrain cerebral ischemic models (Kuang X et al.,2006).

Accordingly, in the present study we evaluated the potential therapeutic effects of LIG post-treatment

JPET Fast Forward. Published on March 11, 2011 as DOI: 10.1124/jpet.110.177055
This article has not been copyedited and formatted. The final version may differ from this version.

following SAH brain injury. Specifically hypothesizing that treatment with LIG may reduce brain injury by altering key players in the apoptotic pathway. In order to carry-out our experiment, various parameters were studied including neurobehavioral function, brain water content, blood-brain barrier permeability, histopathological changes, and evaluation of pro- and/or anti-apoptotic protein expression.

JPET Fast Forward. Published on March 11, 2011 as DOI: 10.1124/jpet.110.177055
This article has not been copyedited and formatted. The final version may differ from this version.

Methods

Animals

All animal experiments were performed in accordance with China Animal Welfare Legislation and were approved by the Chongqing Medical University Committee on the Care and Use of Laboratory Animals. Adult male Sprague-Dawley (SD) rats (n=215) weighing 230 to 310g were purchased from the Animal Center of Chongqing Medical University. The rats were housed in light and temperature controlled environments with food and water available *ad libitum*.

Isolation of Z-Ligustilide

Radix Angelica sinensis was purchased from its cultivating base at the Good Agricultural Practice in Min Xian County, Gansu Province, P.R. China. Its identity was confirmed by comparison with descriptions of characteristics and the appropriate monograph in the Chinese Pharmacopoeia 2000. LIG was prepared as previously described (Kuang X et al, 2006). Briefly, *Angelica sinensis* essential oil was extracted using supercritical-CO_2 fluid. LIG was isolated from the oil by silica gel column chromatography and identified by electron impact ionization mass spectrometry, ^{1}H nuclear magnetic resonance, and ^{13}C nuclear magnetic resonance spectrometry. Purity was determined to be >98% based on the percentage of total peak area by gas chromatography. LIG was prepared with 3% Tween-80 before use.

SAH Model

Experimental SAH was induced using a modified rat double hemorrhage model as previously reported (Lee JY et al., 2008). Briefly, male SD rats were anesthetized with chloral hydrate intraperitoneally at a dose of 350 mg/kg. Throughout the surgery, animals were allowed to breathe spontaneously while a rectal temperature

JPET Fast Forward. Published on March 11, 2011 as DOI: 10.1124/jpet.110.177055
This article has not been copyedited and formatted. The final version may differ from this version.

was maintained at approximately 37±0.5℃ using a homeothermal operating table. After proper positioning in a stereotactic frame, a parieto-occipital incision was made. The nuchal muscle layers were then divided - exposing the atlanto-occipital membrane. The cisterna magna was punctured using a 27-gauge needle, and 0.1 ml of cerebral spinal fluid was gently aspirated. Non-heparinized autologous blood (0.1 ml/100 g) from the femoral artery was injected aseptically into the cisterna magna over a period of 2 min to induce the first SAH. The needle was left in place for an additional 30 min after injection to prevent the possible leakage of blood. After removal of the needle, the skull hole was closed with glue. To permit blood distribution around the basal arteries, the rats were tilted 30° for 30 min with the head down position. After the animals recovered from the effects of anesthesia, they were returned to their cage in a room where the temperature was maintained at 24 to 26°C. The same procedure was repeated 48 h after the first induction of SAH and 0.2 ml of autologous blood injected to induce the second SAH. Sham operated rats received two intracisternal injections of equal volume of physiological saline solution according to the same procedure.

Experimental protocol

Male SD rats (n=215) were randomly assigned to the following weight-matched groups: (1) Sham group (surgery without SAH insult, n=40); (2) SAH+vehicle group (SAH insult, treated with vehicle, n=61); (3) SAH+LIG5 group (SAH insult, treated with LIG 5 mg/kg, n=60); and (4) SAH+ LIG20 group (SAH, treated with LIG 20 mg/kg, n=54). Thirty minutes after the first SAH, SAH+LIG5 and SAH+LIG20 group received intravenous injections of LIG administered at doses of 5 and 20 mg/kg via vena caudalis. No treatment was applied in the sham-operated group while the SAH+vehicle groups were treated with a volume-matched vehicle (3% Tween-80). All treatments were given at the same time point for the next 7 days. Animals that died either on the table or within the first 3 hours following operation had not been allocated to any group. The animals that

died after surgery were replaced until the final group size reached an expected number in each group. The algorithm of the experimental protocol is summarized in Figure 2.

Mortality

Mortality was calculated on day 7 after the first blood injection. The animals that were expected to be sacrificed on day 3 were not included in the mortality calculation. The number of animals in each group designated for the mortality study were Sham (n=27), SAH+vehicle (n=33), SAH+LIG5 (n=32), and SAH+LIG20 (n=29).

Neurobehavioral Testing

Neurobehavioral testing was performed as previously described by Lee et al (Lee JY et al., 2008). Briefly, animal subjects were observed for 5 min in a normal cage environment by two treatment-blinded investigators. Neurobehavioral condition was scored as the following: Grade 1—no deficit, i.e., the rat moved around, explored the environment within a short period of time and approached at least three walls of the cage without motor deficits; Grade 2—slightly affected, i.e., the rat moved about in the cage with a delay but did not approach all sides and hesitated to move, although it eventually reached at least one upper rim of the cage; Grade 3—moderately affected, i.e., the rat did not rise up at all and barely moved in the cage without abnormality; Grade 4—severely affected, i.e., the rat did not move at all, and showed tetra- or paraplegia. The first evaluation (day 0) was performed 6h following the first SAH. Additional neurobehavioral testing was completed at the same time points on each follow-up day.

Brain Water Content

JPET Fast Forward. Published on March 11, 2011 as DOI: 10.1124/jpet.110.177055
This article has not been copyedited and formatted. The final version may differ from this version.

Rats were sacrificed on day 3 and day 7 for brain water content evaluation. The brains were harvested and separated into two parts: cerebrum and cerebellum. The cerebellum was used as an internal control for brain water content. Each brain sample was weighed immediately after removal (wet weight) and weighed again after drying in an oven at 105°C over 24 h (dry weight) as described previously (Xi G et al., 2001). Brain water content (%) was calculated as [(wet weight - dry weight)/ wet weight] × 100.

Blood-Brain Barrier Permeability Assessment

To determine effects of LIG on blood-brain barrier (BBB) permeability, brains were harvested on day 3 and day 7. BBB permeability was assessed by quantifying Evans blue (EB) dye extravasations as described by Mikawa et al. (Mikawa S et al., 1996). The animals were injected intravenously via the caudal vein with 4 ml/kg of 2% (w/v) EB dye and, 60 min later, perfused with physiological saline solution through the left ventricle until the drainage was colorless. Afterwards, each brain was dissected, weighed and homogenized in 3.5 ml of phosphate-buffered saline and vortex-mixed for 2 min after the addition of 2.5 ml of 60% trichloroacetic acid. After a centrifugation for 30 min at 1000 rpm, the absorbance of the supernatants for EB dye was measured at 610 nm with a spectrophotometer (UV-7504, Shanghai Precision Company, China). EB dye content is expressed as μg/g of brain tissue against a standard curve.

Histological Examination

A series of studies was undertaken to examine the caliber and morphology of the basilar artery (BA) following SAH. The rats were sacrificed on day 7 and then intracardially perfused with cold physiological saline solution followed by 4% paraformaldehyde as described previously (Gules I et al., 2002). The brains were immediately removed and post-fixed in the same fixative solution for 24 h.

The specimens for the light microscope study were dehydrated in graded ethanol, embedded in paraffin, sectioned, and stained with hematoxylin and eosin. Diameter and lumen cross-sectional areas of BA were determined and calculated as described previously with slight modifications (Gules I et al., 2002). Light microscopic sections of arteries were projected as digitized video images. The inner perimeters of the vessels were measured by tracing the luminal surface of the intima and the radii (r) were calculated (r=measured inner perimeter /2π). Based on the calculated r value, we calculated the area of a generalized circle (area=πr^2) and then averaged the resultant values to correct for any vessel deformation. The thickness of the vessel wall was measured as the distance from the luminal surface of the intima to the outer border of the media at four different points of each artery, so as not to include the adventitia. Those four measurements were averaged for one score. An independently treatment-blinded investigator took the measurements.

Electron microscopy

For transmission electron microscopy studies, the rats were sacrificed on day 7 and intracardially perfused with cold physiological saline solution followed by 4% paraformaldehyde and 2.5% glutaraldehyde in 0.1M phosphate buffer solution (0.1M PBS, pH7.4). After perfusion, the whole brain was removed and post-fixed overnight in the same fixative. BA were dissected out from the brain and placed in buffered 1% osmium tetroxide for 2 h and washed in 0.1M PBS. Afterwards, specimens were dehydrated in graded ethanol, embedded in epon-araldite epoxy resin, sectioned, and examined by a TOSHIBA 7005 transmission electron microscopy.

Immunohistochemistry

Tissue preparation was conducted as previously noted above. Briefly, coronal sections of the brain were

processed into paraffin blocks and 10 μm slices were cut using a microtome. After dewaxing, the slices were heated and boiled for 30 min in citrate buffer solution (0.01M, pH6.0) for retrieval antigen. Each section was treated with 3% hydrogen peroxide for 20 min at room temperature to diminish nonspecific staining. After rinsing with PBS, the slices were blocked with 5% normal goat serum in PBS (0.1M, pH 7.4) for 30 min at room temperature. The slices were then incubated with the primary antibody (rabbit anti-Bcl-2 (1:100), rabbit anti-Bax (1:200), rabbit anti-p53 (1:100)) (Santa Cruz Biotechnology, Santa Cruz, CA, USA), and rabbit anti-cleaved Caspase-3 (1:100) (Cell Signaling Technology, Danvers, MA, USA)) overnight at 4℃. After rinsing with PBS, the specimens were incubated with biotinylated secondary antibody at room temperature for 30 min, and then re-incubated with peroxidase-labeled streptavidin for 15 min. The immunoreactivity was visualized by 3, 3′-diaminobenzidine tetrahydrochloride solution. For the negative control, some slices from each group were incubated in a medium omitting the primary antibody. After counterstained with hematoxylin, slices were dehydrated and cover-slipped.

TUNEL Staining

Coronal brain slices were stained using the TdT-mediated dUTP-biotin nick end labeling (TUNEL) staining kit (Roche Inc., Basel, Switzerland) to evaluate apoptotic neuronal cells. Cells showing nuclear condensation or fragmentation and apoptotic bodies in the absence of cytoplasmic TUNEL reactivity were considered as apoptotic neuronal cells. The apoptosis index was calculated as previously described (Wang L et al., 2005).

Western Blotting

Under deep anesthesia, rats were perfused intracardially with 200 ml ice-cold physiological saline

solution on day 7. The cerebral cortex was isolated and homogenized for 30 min in radio-immunoprecipitation assay lysis buffer with phenylmethylsulfonyl fluoride. The insoluble material was removed by centrifugation at 12 000 g for 15 min. 50 μg of each lysate sample was denatured for 5 min in sample buffer and was separated by 10% SDS-PAGE. After electrophoretic transfer of the separated polypeptides to the polyvinylidene difluoride membranes at 100 V for 90 min, the membranes were blocked with 1% bovine serum albumin in Tween-TBS (TBST) for 1h at room temperature. The membranes were then incubated with the primary antibody at 4℃ overnight. The following primary antibodies were used: anti-p53 antibody (1:500), anti-Bax(1:500), anti-Bcl-2(1:500), anti-β-actin(1:500) (Santa Cruz Biotechnology, Santa Cruz, CA, USA) and anti-cleaved-caspase-3 (1:1000) (Cell Signaling Technology, Danvers, MA, USA), respectively. The membranes were probed with horseradish peroxidase-conjugated anti-rabbit secondary antibody (1:2000) (Santa Cruz Biotechnology, Santa Cruz, CA, USA) for 1h at room temperature. The immunoreactive bands were visualized using an enhanced chemiluminescence method and were quantified by Quantity One Software (Biorad, Hercules, CA, USA). As a loading control, β-actin was blotted on the same membranes after stripping (Nakamura Y., 2004). The number of animals in each group used for Western blot analysis was five.

Statistical analysis

SPSS software (version 10.0) was used for all statistical calculations. All data are expressed as mean±standard deviation. The statistical significant of differences between means was evaluated by the one way analysis of variance (ANOVA) followed by the Student-Newman-Keuls (SNK) test for multiple comparisons. A probability value of $p < 0.05$ was considered statistically significant.

JPET Fast Forward. Published on March 11, 2011 as DOI: 10.1124/jpet.110.177055
This article has not been copyedited and formatted. The final version may differ from this version.

Results

Mortality

Out of 215 total rats, 39 died either on the table or within the first 3 hours following operation. These animals were excluded from further analysis. The mortality on day 7 after the second SAH was 21.21% (7 of 33) in SAH+vehicle group, 18.75% (6 of 32) in SAH+LIG5 group, 10.34% (3 of 29) in SAH+LIG20 group, and 3.70% (1 of 27) in the sham group.

Neurobehavioral evaluation

Generally speaking, neurobehavioral deficits were encountered in all SAH injured groups and were characterized by lethargy, drowsiness, and minimal movements. The neurobehavioral scores revealed worst scores for every group at 6 hours following the first SAH (day 0) and the second SAH (day 2). Although neurobehavioral scores in all SAH groups were poor between day 3 and day 5, the scores in the SAH+LIG20 group significantly improved compared to the SAH+vehicle and SAH+LIG5 groups on day 3 and 4 (Fig. 3). After day 5, all animals showed a rapid improvement in their neurobehavioral status.

Brain Water Content

Brain edema as indicated by increased brain water content, was seen at 24 h after the 2nd SAH (day 3). In the SAH+vehicle group, the brain water content increased significantly compared with the sham group (79.12%±0.23% vs 78.34%±0.40%, p <0.01). This increase was significantly reduced on day 3 with LIG20 therapy (78.66%±0.35% vs 79.12%±0.23%, p <0.05). The administration of LIG (5 mg/kg) did not reduce brain edema at this time point (78.94%±0.18% vs 79.12%±0.23%, p >0.05). On day 7, there was no significant difference among the groups (Figure 4).

BBB Permeability

The BBB analysis showed a significant protection afforded by LIG (20 mg/kg) on day 3 compared with the SAH+vehicle group. The value of EB dye extravasations in the SAH+vehicle group was significantly higher than that in the sham group (9.05±2.48 vs 3.86±1.14 μg/g, p <0.01) and SAH+LIG20 group (9.05±2.48 vs 5.65±1.04 μg/g, p <0.05). Low dose (5 mg/kg) treatment failed to produce a significant difference. On day 7, there was not a significant difference among the four groups (Fig. 5).

Cerebral Vasospasm

Representative pictographs of the BA can be seen in Figure 6A. No vasospasm was noted in the sham group animals (Fig. 6A-d). However, severe morphological vasospasm was observed in the SAH+vehicle groups (Fig. 6A-a), characterized by corrugation of the internal elastic lamina and contraction of the smooth muscle cells. In addition, the vessel lumen was decreased in size and the vessel wall thickness was increased. A dose-dependent improvement was found in the BA treated with 5 or 20 mg/kg LIG (Fig. 6A-b and c).

The average cross-sectional area of the basilar artery in the SAH+vehicle group was 12411.93±2008.04 μm^2, which was increased to 13417.14±3690.16 μm^2 (p>0.05) and 18092.23±4270.35 μm^2 (p<0.05) with 5 and 20 mg/kg LIG treatment (Figure 6B). The average wall thickness of the basilar artery in SAH+vehicle, SAH+LIG5, SAH+LIG20, and sham groups was 25.91±10.65 μm, 27.51±7.37 μm, 15.69±5.22 μm, and 14.42±4.09 μm, respectively (Fig. 6C). The wall thickness in SAH+LIG20 (p<0.05) and sham (p<0.05) group was significantly greater than that in the SAH+vehicle group.

Ultrastructural Appearances

Representative ultrastructural micrograms of the basilar arteries obtained from the SAH+vehicle, SAH+LIG20, and sham group are shown in Figure 7. The endothelial cells in the sham group were flat and spindle in shape, tightly attached to the internal elastic lamina, and characterized by a single continuous layer of contacts of varying length with tight junctions and occasional indentations. The smooth muscle cells were glabrous without corrugation. There was no vacuolization in either endothelial or smooth muscle cells (Fig. 7c). Pathomorphological changes were observed in the SAH+vehicle group on day 7. These changes include swelling, vacuolization, disorientation and desquamation of endothelial cells, disruption of tight junctions, and widening interendothelial spaces. Prominent corrugation was also noted in the internal elastic lamina and smooth muscle cells (Fig. 7a). In animals with SAH, treatment with high-dose LIG (20 mg/kg) attenuated damage to endothelial cells and released elastic lamina and smooth muscle contracture (Fig. 7b).

TUNEL Staining

Sporadic TUNEL-positive cells were detected in the sham group. On day 7, TUNEL-positive cells appeared in the brain cortex of SAH+vehicle and SAH+LIG5 groups. A remarkably lesser degree of TUNEL-positive staining in the cortex was shown in the SAH+LIG20 group (Fig. 8). The apoptosis index in SAH+vehicle, SAH+LIG5, SAH+LIG20, and sham groups was 52.96%±7.29%, 49.77%±6.83%, 39.68%±5.73%, and 7.49%±7.03%, respectively (SAH+LIG20 and sham vs SAH+vehicle group, $p<0.01$).

Apoptosis-Related Protein Expression

To further explore the potential mechanisms involved in apoptosis inhibition following LIG treatment, the expression of pro-apoptotic proteins (p53, cleaved caspsase-3, and Bax) and anti-apoptotic protein (Bcl-2) were investigated using the immunohistochemical method (Fig. 9). The findings showed that the

immunoactivity of p53 and cleaved caspase-3 was very weak in the brain tissues of the sham group while SAH brain injury resulted in a significant increase in the expressions of both proteins. An obvious down-regulation of p53 and cleaved caspase-3 expressions were found in the SAH rats treated with 20 mg/kg LIG. Although SAH up-regulated the Bax expression in the brain, treatment with either 5 or 20 mg/kg LIG had no effect on the protein expression. The level of anti-protein Bcl-2 was reduced after SAH, and was dose-dependently up-regulated following treatment with 5 or 20 mg/kg LIG.

To quantify the expression of the apoptosis-related proteins, protein levels of p53, Bax, Bcl-2, and cleaved caspase-3 in the cortex were measured using western blot analysis (Fig. 10). The results from western blotting were similar to the findings from immunohistochemistry.

JPET Fast Forward. Published on March 11, 2011 as DOI: 10.1124/jpet.110.177055
This article has not been copyedited and formatted. The final version may differ from this version.

Discussion

Angelica sinensis has been used as a medicinal plant and is included in numerous traditional Chinese herbal prescriptions for thousands of years. Besides being used to modulate the immune system, treat obstetrical and gynecological disorders and prevent platelet aggregation, it has been clinically administered to treat cerebrovascular and cardiovascular diseases. Previous studies show that the effective constituents of *Angelica sinensis* extract are classified into water soluble part and essential oil. The former including polysaccharides and ferulic acid is widely used in clinic. The effective substances of the essential oil are still largely unknown. It has been reported recently that Z-Ligustilide (LIG) is one of the major essential oil components and characteristic phthalide component of *Angelica sinensis*. It has numerous pharmacological actions, including antiasthmatic and analgesic effects, antiproliferative effects on smooth muscle cells, improved microcirculation and smooth muscle relaxation. Multiple studies have reported that LIG provided significant neuroprotective effects on transient forebrain ischemia in mice (Kuang X et al., 2006), permanent forebrain ischemia in rats (Kuang X et al., 2008) and focal cerebral ischemia in rats (Peng HY et al, 2007). However, much less is known about the potential effects of LIG on brain injury following SAH.

The aim of this study was to evaluate the potential therapeutic use of LIG as a treatment option following a subarachnoid hemorrhage (SAH) brain injury. We were able to show for the first time that LIG post-treatment could provide effective neuroprotection against SAH by reducing apoptotic damage through decreased expression of p53 and cleaved caspase-3, and in doing so, subsequently limit the formation of secondary brain injuries. Specifically, we found that it reduced mortality amongst our rat population, increased neurobehavioral scores, and decreased both BBB permeability and brain edema. In addition, post-treatment reduced cerebral vascular wall thickness, increased vessel diameter, and improved the histological appearance of vascular endothelial cells within the basilar artery walls.

Secondary brain injury as a result of SAH has been recognized as a leading cause of death and disability in patients (Bederson JB et al., 1995). These injuries include brain edema formation, cerebral arterial vasospasm, BBB disruption, and neurobehavioral deficits. Recently, mounting evidence has suggested that apoptosis may be the key orchestrator of secondary brain injury following SAH (Cahill J et al., 2006). Therefore, therapeutic agents that can block and/or slow down the activation of apoptotic signals can translate into reduced short and long-term clinical outcomes. In the present study, we found that TUNEL-positive cell counts, which are a strong marker for neuronal cell death, were significantly increased following SAH injury and could be effectively reduced following LIG treatment. Specifically, we were able to demonstrate a markedly elevated expression of p53 following SAH injury which was reduced following treatment. This is important because p53, a well-known tumor suppression protein, has been implicated in a host of intracranial pathologies, including cerebral ischemia and Alzheimer's disease (Daily D et al., 1999; Mattson MP, 2000; Leker RR et al., 2004; Cahill J et al., 2007), and has been shown to orchestrate the development of vasospasm and neuronal cell death following SAH injury (Zhou C et al., 2004; Zhou C et al., 2005; Cahill J et al., 2007).

Other key players in the apoptotic cascade are members of the Bcl family, which are important endogenous regulators in the mitochondrial apoptotic pathway (Oltvai ZN et al., 1993). Cell survival during the apoptotic cascade depends on the balance between the pro- and anti-apoptotic proteins of this family. Bax, a pro-apoptotic protein, and Bcl-2, an anti-apoptotic protein, are the two primary members of the Bcl-2 family (Perfettini 2002, Antonsson 2001, Gross 1999, Tsujimoto 2003). This is important because one of the largest target groups of p53 is the Bcl-2 family. A growing body of evidence suggests that p53 can function as a direct transcriptional activator of Bax and may either directly or indirectly down-regulate expression of the Bcl-2 gene via a p53-dependent negative response element. The inhibition of p53 allows for the balance of pro- to anti-apoptotic members of the Bcl-2 family to tip in favor of survival, thereby preventing mitochondrial pore

formation and, ultimately, the release of apoptosis-promoting factors. (Miyashita T et al., 1994a; Miyashita T et al., 1994b; Miyashita T and Reed JC, 1995) In our study, we found that the immuno-reactivity of Bcl-2 was decreased in brain regions following SAH injury, while Bax expression was increased. Although treatment with LIG in the SAH group did not influence Bax expression following injury, it resulted in a dose-dependent increase in Bcl-2 levels, which led to a large shift of Bcl-2/Bax ratio in favor of the anti-apoptotic Bcl-2. In fact, some studies have shown that the Bcl-2/Bax ratio may be a stronger predictor of apoptotic activity than the concentrations of either Bax or Bal-2 alone (Oltvai ZN et al, 1993).

Caspase-3 is a downstream member of the caspase-dependent apoptotic pathway. The decrease of Bcl-2/Bax ratio may initiate apoptosis by causing the loss of outer mitochondrial membrane integrity. This results in the release of apoptogenic proteins such as cytochrome C from the intermembrane space of mitochondria. The released cytochrome C leads to the formation of the apoptosome complex, which, in turn, activates downstream caspases such as caspase-3. Furthermore, activated caspase-3 cleaves numerous nuclear enzymes associated with apoptosis such as PARP. So caspase-3 is considered one of the central effector of apoptosis. Previous studies have alluded to the role of caspase-3 in cortical neuron apoptosis post-SAH (Park S et al., 2004). In the current study, we found that the cleaved caspase-3 level decreased treatment of LIG resulted in a dose-dependent reduction in cleaved caspase-3 production in cortex following SAH and that this was reversed with LIG treatment after SAH. Thus, the present data suggests that the neuroprotection of LIG treatment after SAH is likely associated with the shift of Bcl-2/Bax ratio in favor of Bcl-2, resulting in decreased activation of caspase-3 in cortical neuron post-SAH.

Although upstream regulators of these apoptotic proteins were not detected in the present study, previous studies have investigated actions of LIG on some regulators in other models. A study of LIG in vascular smooth muscle cells demonstrated that LIG had the potential to suppress ERK1/2, p38, and JNK, the members of

mitogen-activated protein kinases (MAPKs) in associated with decreased intracellular reactive oxygen species (ROS) production, which resulted in inhibition of vascular smooth muscle cells proliferation and cell cycle progression (Lu Q et al., 2006). Moreover, a recent study showed that pretreatment of the PC12 cells with LIG significantly attenuated H_2O_2-induced cell death via reducing increased intracellular ROS levels, downregulation of Bax, cleaved-caspase 3, and cytochrome-c expression, and upregulation of Bcl-2 expression (Yu Y et al., 2008). Based on these observations, we could reasonably speculate that LIG treatment might act as a ROS or MAPKs inhibitor to alter the levels of apoptotic proteins, and then promote survival of cortical neurons after SAH. To elucidate the mechanisms of LIG altering apoptotic proteins, further studies on effects of LIG treatment on alterations of above-mentioned regulators after SAH are needed.

In addition to apoptosis, cerebral vasospasm (CVS) following SAH is another secondary brain injury complication. Although the pathogenesis of cerebral vasospasm remains inconclusive, considerable studies have shown that calcium ions play a critical role in almost all stages of CVS formation. Previous research has suggested that LIG treatment can induce vasodilation in the rat mesenteric artery by inhibiting voltage-dependent calcium channels and thus, preventing the receptor-mediated Ca^{2+} influx and release (Cao YX et al., 2006). Similar to these works, our study found that the SAH injured mice had shown traits on H&E staining that were characteristic of SAH induced vasospasm; this included an increase in wall thickness, luminal narrowing, shrunken endothelial cells and corrugation of the internal elastic lamina of the basilar arteries. Moreover, following LIG treatment these changes were notably reduced and additional histogram analysis revealed a significant improvement in cross-sectional area and basilar wall thickness. This suggests that LIG may in fact alter the mechanism responsible for inducing CVS following injury.

In summary, the results of the present study strongly suggest that LIG treatment may in fact ameliorate brain injury following experimental SAH through mechanisms that reduce neuronal apoptosis and subsequently

ameliorate secondary brain injury. Further studies will be needed to determine more mechanistic detail with regards to the role of LIG and apoptosis.

JPET Fast Forward. Published on March 11, 2011 as DOI: 10.1124/jpet.110.177055
This article has not been copyedited and formatted. The final version may differ from this version.

Authorship Contributions

Participated in research design: S. Wang, Chen, and Tang.

Conducted experiments: Chen, Zhu, Li, Jiang, and Tu.

Contributed new reagents or analytic tools: C. Wang.

Performed data analysis: S. Wang, Chen, Tang, Khatibi, Zhu, Li, Jiang and Tu.

Wrote or contributed to the writing of the manuscript: S. Wang, Chen, Tang, and Khatibi.

References

Antonsson B (2001) Bax and other pro-apoptotic Bcl-2 family "killer-proteins" and their victim the mitochondrion. *Cell Tissue Res* **306**:347-361.

Bederson JB, Germano IM, and Guarino L (1995) Cortical blood flow and cerebral perfusion pressure in a new noncraniotomy model of subarachnoid hemorrhage in the rat. *Stroke* **26**:1086–1092.

Cahill J, Calvert JW, Marcantonio S, and Zhang JH (2007) p53 may play an orchestrating role in apoptotic cell death after experimental subarachnoid hemorrhage. *Neurosurgery* **60**:531–545.

Cahill J, Calvert JW, and Zhang JH (2006) Mechanisms of early brain injury after subarachnoid hemorrhage. *J Cereb Blood Flow Metab* **26**:1341–1353.

Cao YX, Zhang W, He JY, He LC, and Xu CB (2006) Ligustilide induces vasodilatation via inhibiting voltage dependent calcium channel and receptor-mediated Ca2+ influx and release. *Vascul Pharmacol* **45**:171-176.

Daily D, Barzilai A, Offen D, Kamsler A, Melamed E, and Ziv I (1999) The involvement of p53 in dopamine-induced apoptosis of cerebellar granule neurons and leukemic cells overexpressing p53. *Cell Mol Neurobiol* **19**:261–276.

Janjua N and Mayer SA (2003) Cerebral vasospasm after subarachnoid hemorrhage. *Curr Opin Crit Care* **9**:113-l l9.

Gross A, McDonnell JM, and Korsmeyer SJ (1999) Bcl-2 family members and the mitochondria in apoptosis. *Genes Dev* **13**:1899-1911.

Gules I, Satoh M, Clower BR, Nanda A, and Zhang JH (2002) Comparison of three rat models of cerebral vasospasm. *Am J Physiol Heart Circ Physiol* **283**:H2551–H2559.

Kuang X, Yao Y, Du JR, Liu YX, Wang CY, and Qian ZM (2006) Neuroprotective role of Z-ligustilide against forebrain ischemic injury in ICR mice. *Brain Res* **1102**:145-153.

Kuang X, Du JR, Liu YX, Zhang GY, and Peng HY (2008) Postischemic administration of Z-Ligustilide ameliorates cognitive dysfunction and brain damage induced by permanent forebrain ischemia in rats. *Pharmacol Biochem Behav* **88**:213-221.

Lee JY, Huang DL, Keep R, and Sagher O (2008) Characterization of an improved double hemorrhage rat model for the study of delayed cerebral vasospasm. *J Neurosci Methods* **168**: 358-366.

Leker RR, Aharonowiz M, Greig NH, and Ovadia H (2004) The role of p53-induced apoptosis in cerebral ischemia: effects of the p53 inhibitor pifithrin alpha. *Exp Neurol* **187**:478–486.

Liu J, Burdette JE, Xu H, Gu C, van Breemen RB, Bhat KP, Booth N, Constantinou AI, Pezzuto JM, Fong HH, Farnsworth NR, and Bolton JL (2001) Evaluation of estrogenic activity of plant extracts for the potential treatment of menopausal symptoms. *J Agric and Food Chem* **49**:2472–2479.

Lu Q, Qiu TQ, and Yang H (2006) Ligustilide inhibits vascular smooth muscle cells proliferation. *Eur J Pharmacol* **542**:136-140.

Mattson MP (2000) Apoptosis in neurodegenerative disorders. *Nat Rev Mol Cell Biol* **1**:120–129.

Mikawa S, Kinouchi H, Kamii H, Gobbel GT, Chen SF, Carlson E, Epstein CJ, and Chan PH (1996) Attenuation of acute and chronic damage following traumatic brain injury in copper, zinc-superoxide dismutase transgenic mice. *J Neurosurg* **85**:885–891.

Miyashita T, Harigai M, Hanada M, and Reed JC (1994a) Identification of a p53-dependent negative response element in the bcl-2 gene. *Cancer Res* **54**:3131–3135.

Miyashita T, Krajewski S, Krajewska M, Wang HG, Lin HK, Liebermann DA, Hoffman B, and Reed JC (1994b) Tumor suppressor p53 is a regulator of bcl-2 and bax gene expression in vitro and in vivo. *Oncogene* **9**:1799–1805.

Miyashita T and Reed JC (1995) Tumor suppressor p53 is a direct transcriptional activator of the human Bax gene. *Cell* **80**:293–299.

Nakamura Y (2004) Isolation of p53-target genes and their functional analysis. *Cancer Sci* **95**:7–11.

Oltvai ZN, Milliman CL, and Korsmeyer SJ. (1993) Bcl-2 heterodimerizes in vivo with a conserved homolog, Bax, that accelerates programmed cell death. *Cell* **74**:609-619.

Park S, Yamaguchi M, Zhou C, Calvert JW, Tang J, and Zhang JH (2004) Neurovascular protection reduces early brain injury after subarachnoid hemorrhage. *Stroke* **35**: 2412-2417.

Peng HY, Du JR, Zhang GY, Kuang X, Liu YX, Qian ZM, and Wang CY (2007) Neuroprotective Effect of Z-Ligustilide against Permanent Focal Ischemic Damage in Rats. *Biol Pharm Bull* **30**:309-312.

Perfettini JL, Reed JC, Israël N, Martinou JC, Dautry-Varsat A, and Ojcius DM (2002) Role of Bcl-2 family members in caspase-independent apoptosis during Chlamydia infection. *Infect Immun* **70**:55-61.

Raabe A, Zimmermann M, Setzer M, Vatter H, Berkefeld J, and Seifert V (2002) Effect of intraventricular sodium nitroprusside on cerebral hemodynamics and oxygenation in poor-grade aneurysm patients with severe, medically refractory vasospasm. *Neurosurgery* **50**:1006–1014.

Rosenwasser RH, Armonda RA, Thomas JE, Benitez RP, Gannon PM, and Harrop J (1999) Therapeutic modalities for the management of cerebral vasospasm: timing of endovascular options. *Neurosurgery* **44**:975–980.

Shimizu M, Matsuzawa T, Suzuki S, Yoshizaki M, Morita N. (1991) Evaluation of *Angelicae radix* (Touki) by the inhibitory effect on platelet aggregation. *Che Pharm Bull* (Tokyo) **39**:2046–2048.

Tseng MY, Czosnyka M, Richards H, Pickard JD, and Kirkpatrick PJ (2005) Effects of acute treatment with pravastatin on cerebral vasospasm, autoregulation, and delayed ischemic deficits after aneurysmal subarachnoid hemorrhage: a phase II randomized placebo-controlled trial. *Stroke* **36**: 1627-1632.

Tsuchida T, Kobayashi M, Kaneko K, and Mitsuhashi H (1987) Studies on the constituents of Umbelliferae plants. XVI. Isolation and structures of three new ligustilide derivatives from *Angelica acutiloba*. *Cheml Pharml Bull* **35**:4460–4464.

Tsujimoto Y (2003) Cell death regulation by the Bcl-2 protein family in the mitochondria. *J Cell Physiol* **195**:158-167.

Vajkoczy P, Meyer B, Weidauer S, Raabe A, Thome C, Ringel F, Breu V, and Schmiedek P (2005) Clazosentan (AXV-034343), a selective endothelin A receptor antagonist, in the prevention of cerebral vasospasm following severe aneurysmal subarachnoid hemorrhage: results of a randomized, double-blind, placebo-controlled, multicenter phase IIa study. *J Neurosurg* **103**:9–17.

Wilasrusmee C, Kittur S, Siddiqui J, Bruch D, Wilasrusmee S, and Kittur DS (2002) In Vitro immunomodulatory effects of ten commonly used herbs on murine lymphocytes. *J Altern Complement Med* **8**:467–475.

Xi G, Hua Y, Bhasin RR, Ennis SR, Keep RF, and Hoff JT (2001) Mechanisms of edema formation after intracerebral hemorrhage: effects of extravasated red blood cells on blood flow and blood-brain barrier integrity. *Stroke* **32**:2932-2938.

Wang L, Shi JX, Yin HX, Ma CY, and Zhang QR. (2005) The influence of subarachnoid hemorrhage on neurons: an animal model. *Ann Clin Lab Sci* **35**:79-85.

Yu Y, Du JR, Wang CY, and Qian ZM (2008) Protection against hydrogen peroxide-induced injury by Z-ligustilide in PC12 cells. *Exp Brain Res* **184**:307-312.

Zhou C, Yamaguchi M, Colohan AR, and Zhang JH (2005) Role of p53 and apoptosis in cerebral vasospasm after experimental subarachnoid hemorrhage. *J Cereb Blood Flow Metab* **25**:572-582.

Zhou C, Yamaguchi M, Kusaka G, Schonholz C, Nanda A, and Zhang JH (2004) Caspase inhibitors prevent endothelial apoptosis and cerebral vasospasm in dog model of experimental subarachnoid hemorrhage. *J Cereb Blood Flow Metab* **24**: 419-431.

Footnotes

This work was financially supported by the National Basic Research Program of China [NO. 2009CB918300].

JPET Fast Forward. Published on March 11, 2011 as DOI: 10.1124/jpet.110.177055
This article has not been copyedited and formatted. The final version may differ from this version.

Legends for Figures

Fig. 1. Chemical structures of Z-Ligustilide (LIG)

Fig. 2. Schematic illustration of experimental design. The first and the second SAH were induced on day 0 and day 2 respectively. The triangles indicate administration of LIG or vehicle. The body weight and neurobehavioral score were recorded daily from day 0 to day 7. 12 animals in each group were euthanized on day 3 for brain water content and blood-brain barrier permeability assessment. The rest were euthanized on day 7 for brain water content, blood-brain barrier permeability assessment, histology, immunohistochemistry, western blot and TUNEL staining.

Fig. 3. The effects of LIG treatment on neurobehavioral function following SAH brain injury. The spontaneous activity scores in the SAH+LIG20 were significantly better than those in the SAH+vehicle or SAH+LIG5 groups on day 3 and day 4. Data are expressed as the mean ± S.D. for n=26 (*$p < 0.05$, **$p < 0.01$ versus SAH+vehicle group by ANOVA followed by SNK test).

Fig. 4. Effect of LIG on brain water content following SAH brain injury. The water content in the cerebral hemispheres was significantly decreased in the SAH+LIG20 group on day 3 compared with the SAH+vehicle group. There was not a significant difference among these groups on day 7. The cerebellar water content in these groups did not show significant changes on day 3 or day 7 – confirming the internal control. Data are expressed as the mean ± S.D. for n=6 (*$p < 0.05$, **$p < 0.01$ versus SAH+vehicle group by ANOVA followed by SNK test).

JPET Fast Forward. Published on March 11, 2011 as DOI: 10.1124/jpet.110.177055
This article has not been copyedited and formatted. The final version may differ from this version.

Fig. 5. Effect of LIG on Evan's blue extravasations following SAH brain injury.

A. Representative photograph of the leakage of Evan's blue staining. (a) SAH+vehicle group, (b) SAH+LIG5 group, (c) SAH+LIG20 group, and (d) Sham group.

B. LIG (20 mg/kg) preserved the BBB permeability and decreased the leakage of Evan's blue on day 3 compared with the SAH+vehicle group. There was not a significant difference among these groups on day 7. Data are expressed as the mean ± S.D. for n=6 (*$p < 0.05$, **$p < 0.01$ versus SAH+vehicle group by ANOVA followed by SNK test).

Fig. 6. Effect of LIG treatment on cerebral vasospasm following SAH brain injury.

A. Representative photomicrograph of H&E staining of the basilar artery. In the sham group (d), no vasospasm was observed. The increased wall thickness, luminal narrowing, shrunken endothelial cells and corrugation of the internal elastic lamina in basilar arteries were seen in the SAH+vehicle (a) and SAH+LIG5 (b) groups. Decreased vasospasm was demonstrated in SAH+LIG20 group (c). Scale bar, 20 μm.

B and C. Histogram of the average cross-sectional area (B) and the average wall thickness (C) of the basilar artery. There were significant differences in the cross-sectional area and wall thickness of basilar artery in the SAH+vehicle and sham groups. These changes were significantly attenuated by treatment with LIG (20 mg/kg). Data are expressed as the mean ± S.D. for n=7 (*$p < 0.05$, **$p < 0.01$ versus SAH+vehicle group by ANOVA followed by SNK test).

Fig. 7. Ultrastructure of the basilar arteries. The basilar arteries from the sham group showed smooth, intact, and regular endothelial cells without corrugation of the internal elastic lamina or smooth muscle cells (c). The basilar arteries from the SAH+vehicle group showed pathological changes (a). Vacuolization, disorientation

and desquamation of endothelial cells were noted. The internal elastic lamina got thick and convoluted. Prominent contraction was also observed in smooth muscle cells. The basilar arteries from the SAH+LIG20 showed less pathological changes in endothelial cells, elastic lamina, and smooth muscle cells (b).

Fig. 8. Effect of LIG treatment on apoptotic cell death following SAH brain injury.

A. Representative photomicrograph of TUNEL staining in the cortex (arrow indicating TUNEL-positive cells). The sham group (d) showed sporadic TUNEL-positive cells. SAH+vehicle group (a) showed increased TUNEL apoptotic endothelial cells with intense nuclear stained as brown. SAH+LIG20 group (c) showed less TUNEL apoptotic cells than the SAH+vehicle group. Scale bar, 20 μm.

B. Apoptosis index. Treatment with LIG (20 mg/kg) markedly attenuated apoptosis induced by SAH. Data are expressed as the mean ± S.D. for n=7 (**$p < 0.01$ versus SAH+vehicle group by ANOVA followed by SNK test).

Fig.9. Immunohistochemistry staining of p53, Bax, Bcl-2, and cleaved caspasse-3. The immunohistochemical expressions of p53, Bax, and cleaved caspase-3 were elevated while the expression of Bcl-2 was decreased in the SAH+vehicle group. Treatment with LIG (20 mg/kg) reduced the expressions of p53 and cleaved caspase-3 and increased the expression of Bcl-2. LIG had no significant effect on the expression of Bax in cortex after SAH. Scale bar, 20 μm.

Fig.10. Western blot analysis of p53, Bcl-2, Bax, and cleaved caspase-3.

A. Representative immunoblots of p53, Bcl-2, Bax, and cleaved caspase-3 in the cortex following SAH.

B~E. Histogram representing p53, Bcl-2, Bax, and cleaved caspase-3 expressions measured using densitometry

JPET Fast Forward. Published on March 11, 2011 as DOI: 10.1124/jpet.110.177055
This article has not been copyedited and formatted. The final version may differ from this version.

analysis. Data are expressed as the mean ± S.D. with five animals per group normalized to β-actin and expressed as a percentage of the mean value of the sham group (*$p < 0.05$, **$p < 0.01$ versus SAH+vehicle group by ANOVA followed by SNK test).

JPET Fast Forward. Published on March 11, 2011 as DOI: 10.1124/jpet.110.177055
This article has not been copyedited and formatted. The final version may differ from this version.

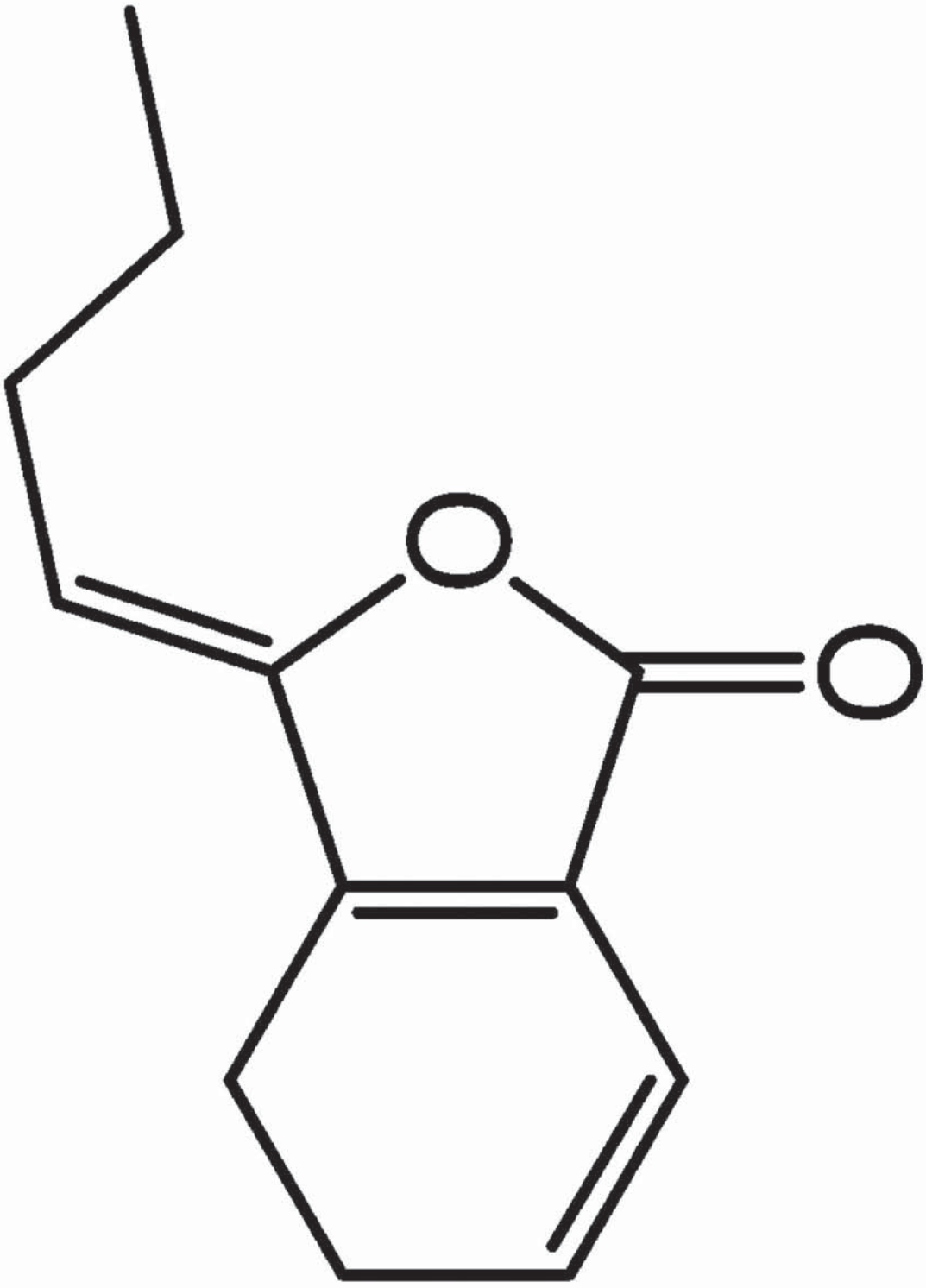

Z-Ligustilide (LIG)

Figure 1

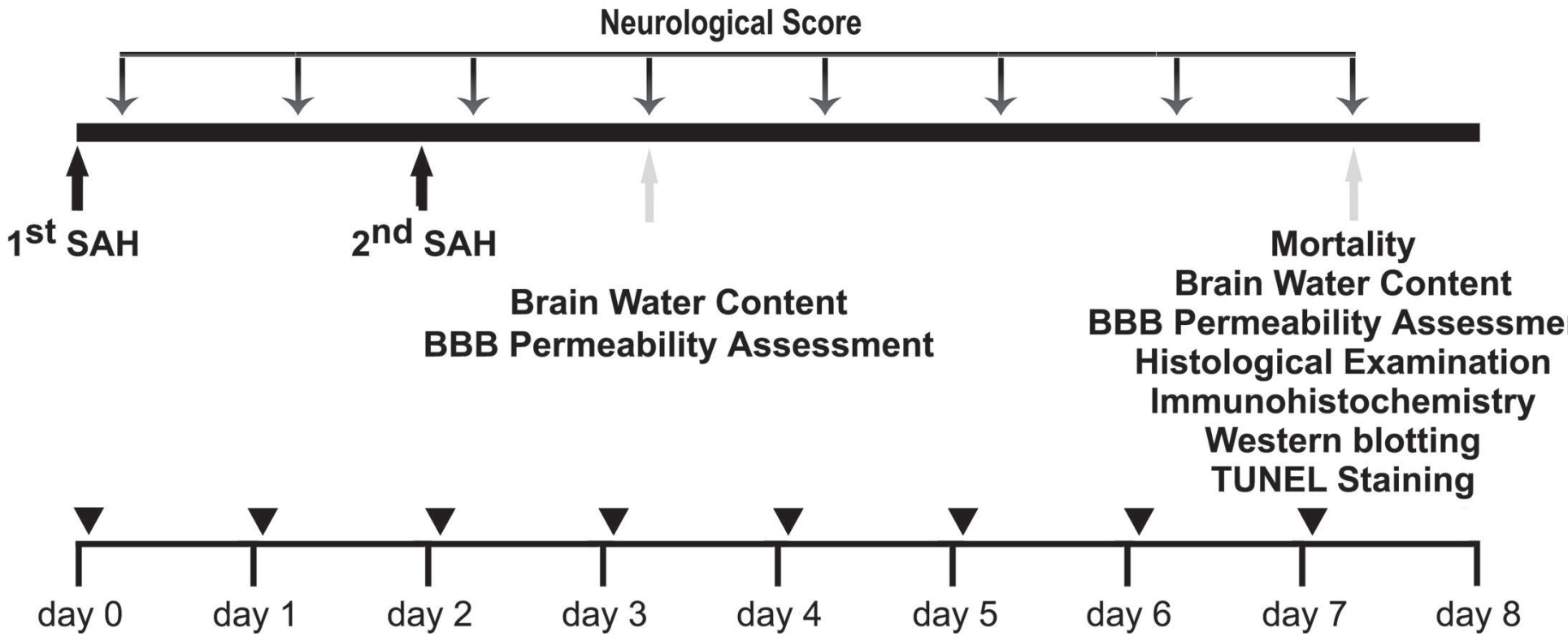

Figure 2

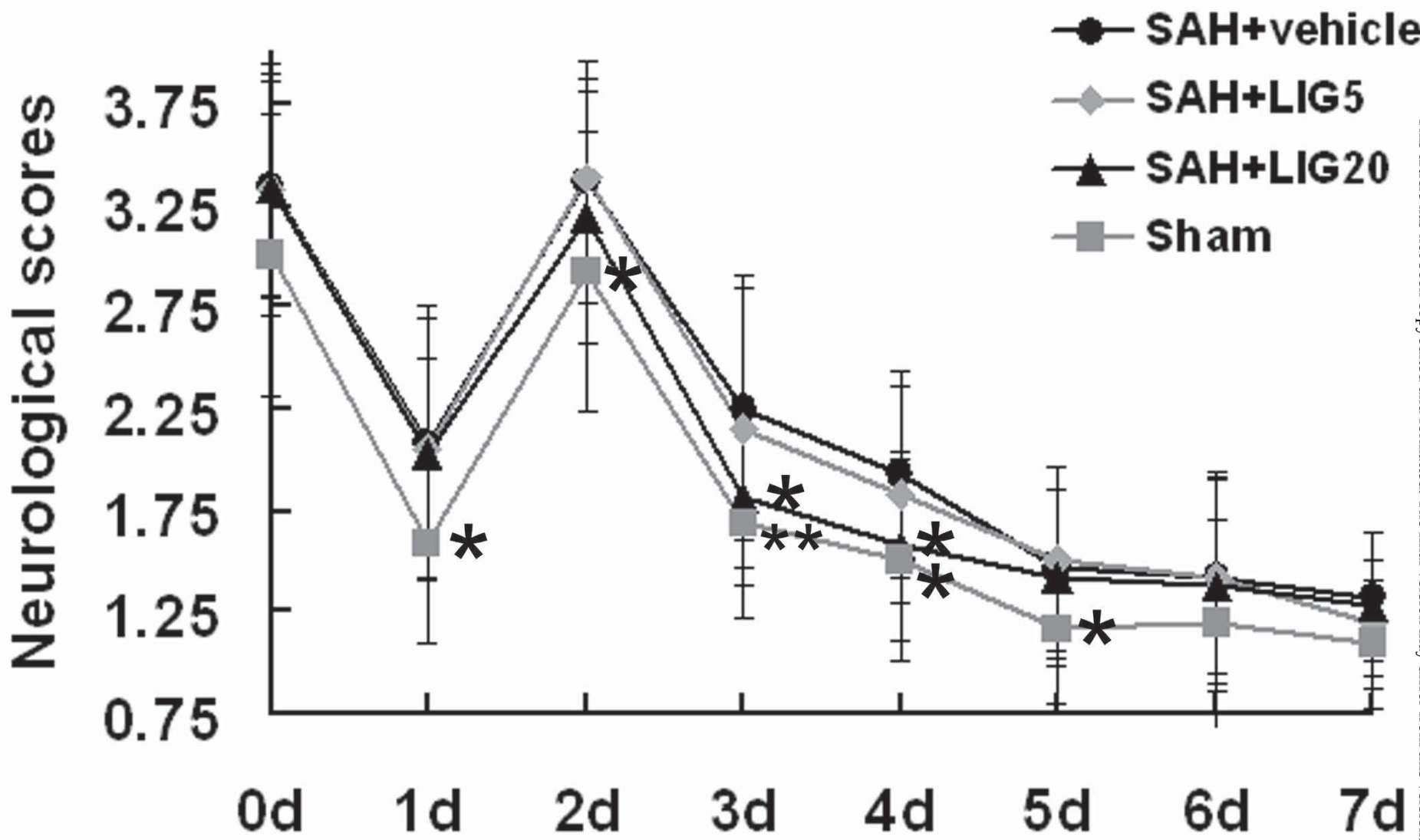

Figure 3

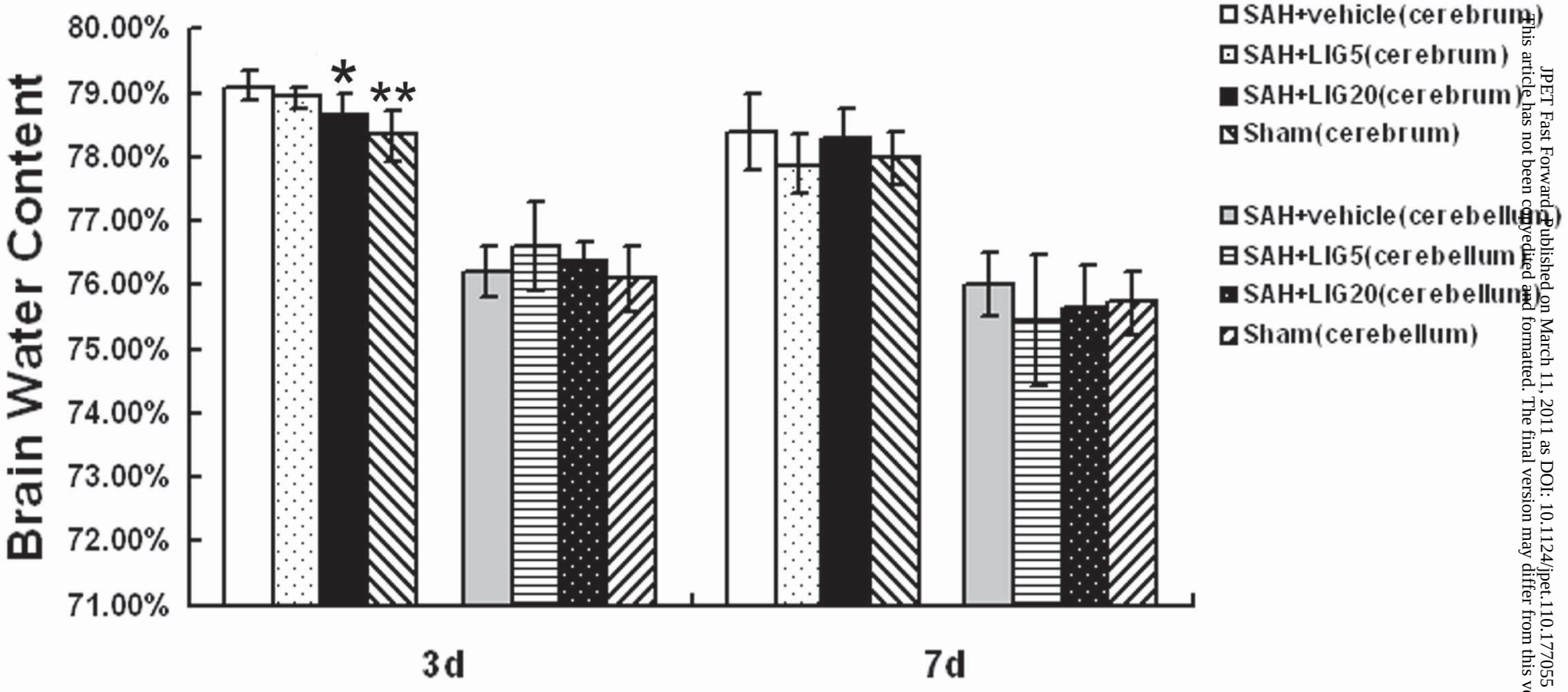

Figure 4

JPET Fast Forward. Published on March 11, 2011 as DOI: 10.1124/jpet.110.177055
This article has not been copyedited and formatted. The final version may differ from this version.

A

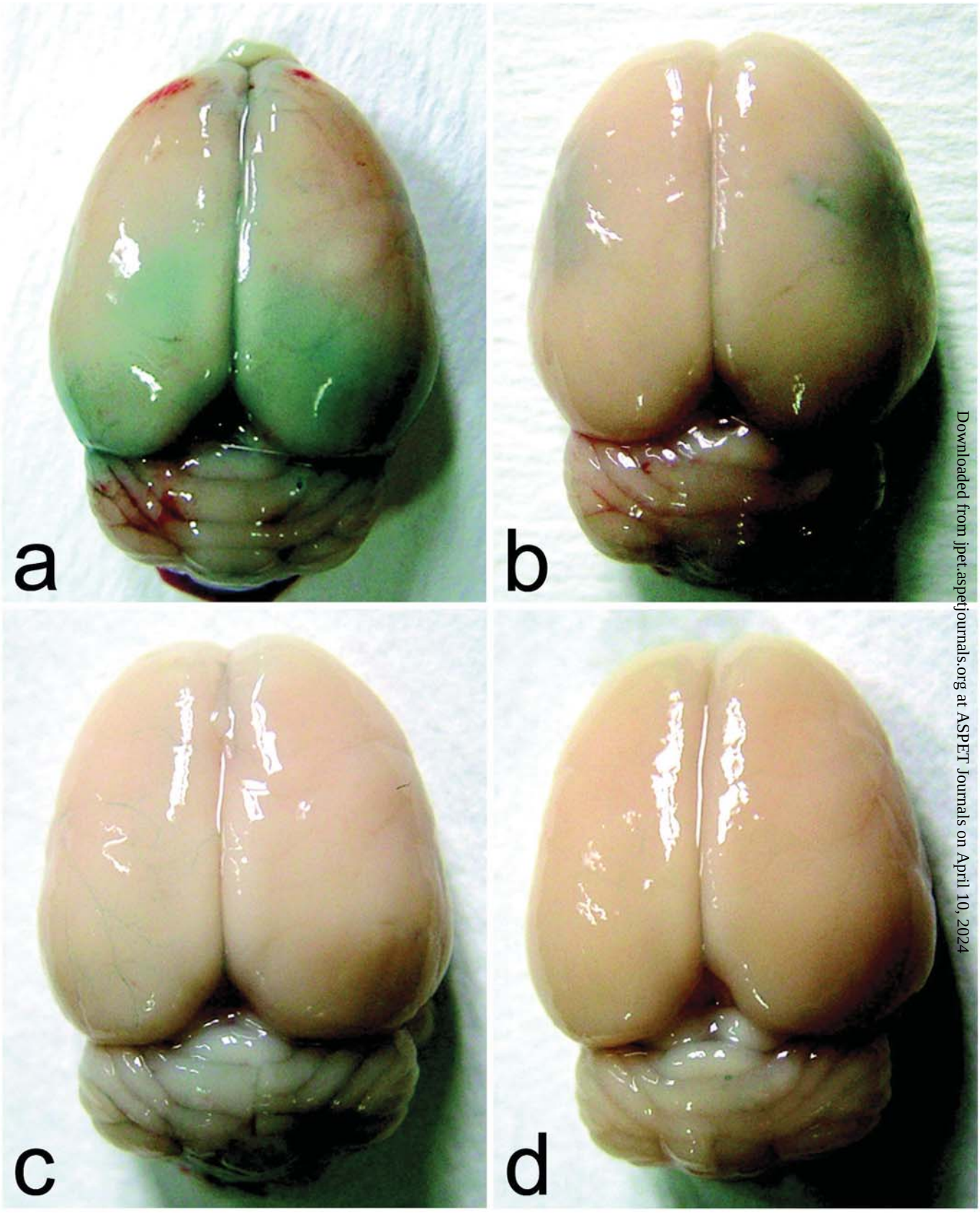

Figure 5

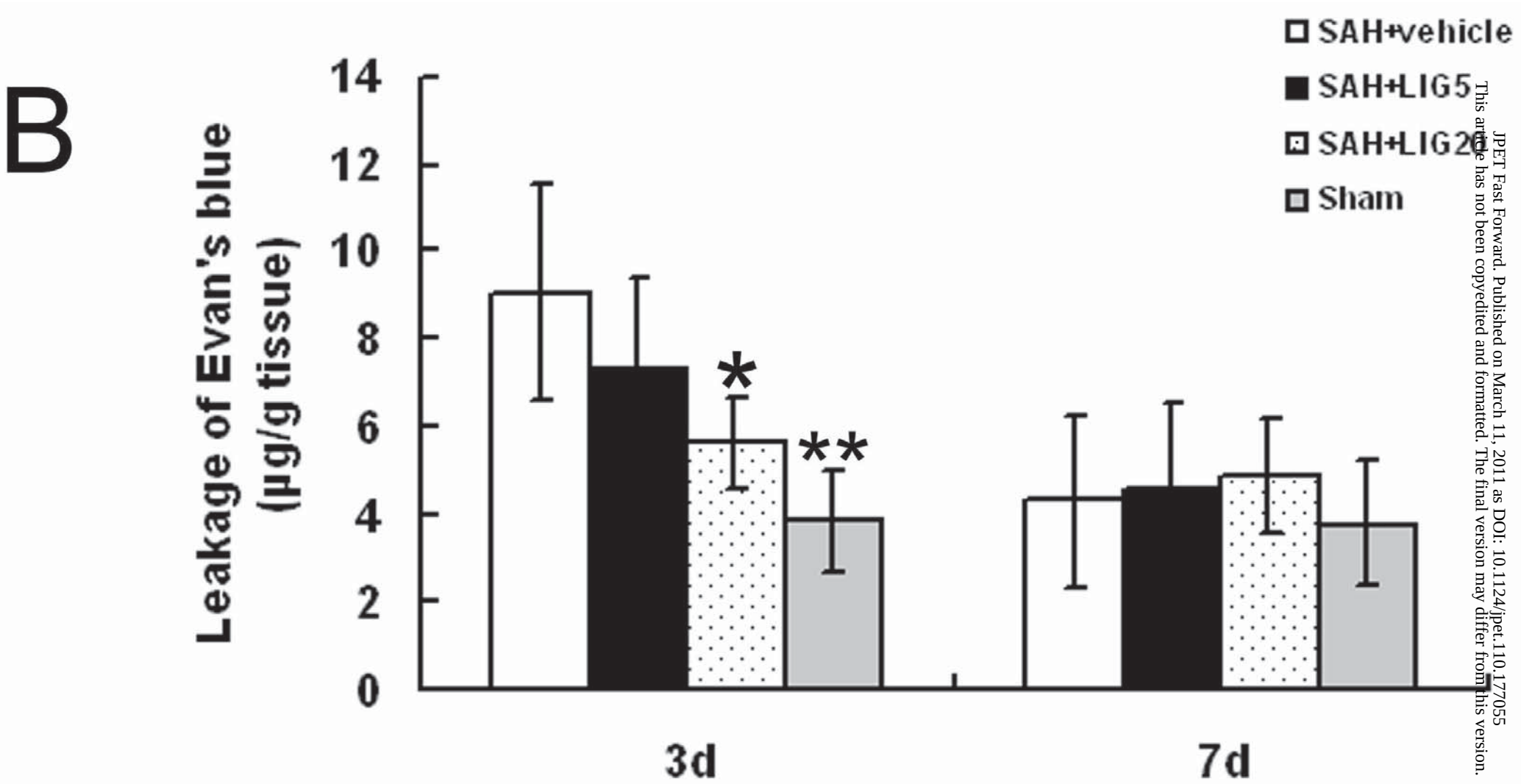

Figure 5

Figure 6

JPET Fast Forward. Published on March 11, 2011 as DOI: 10.1124/jpet.110.177055
This article has not been copyedited and formatted. The final version may differ from this version.

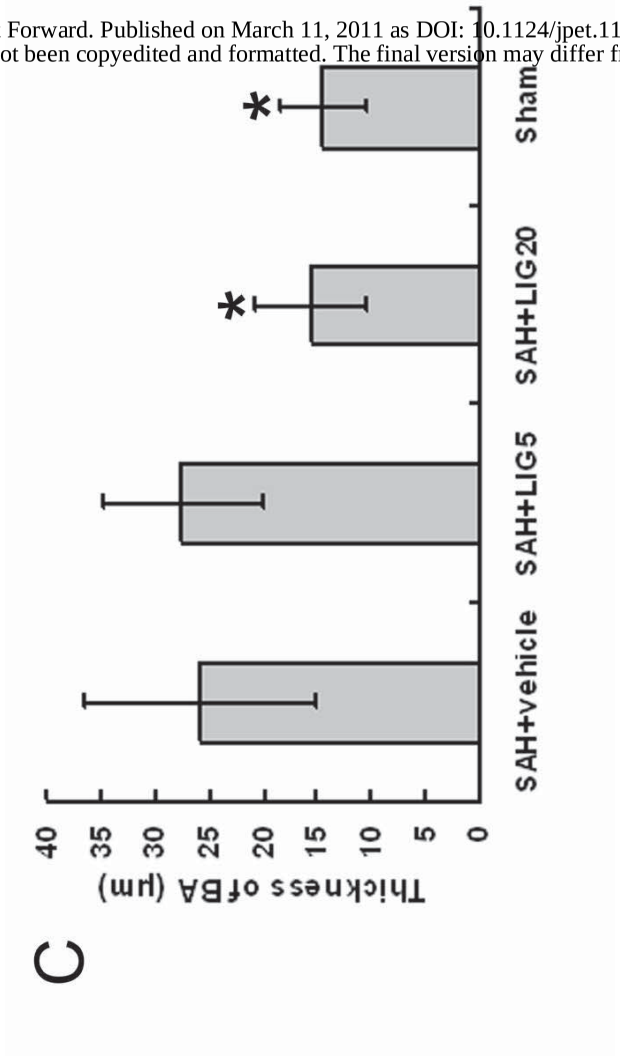

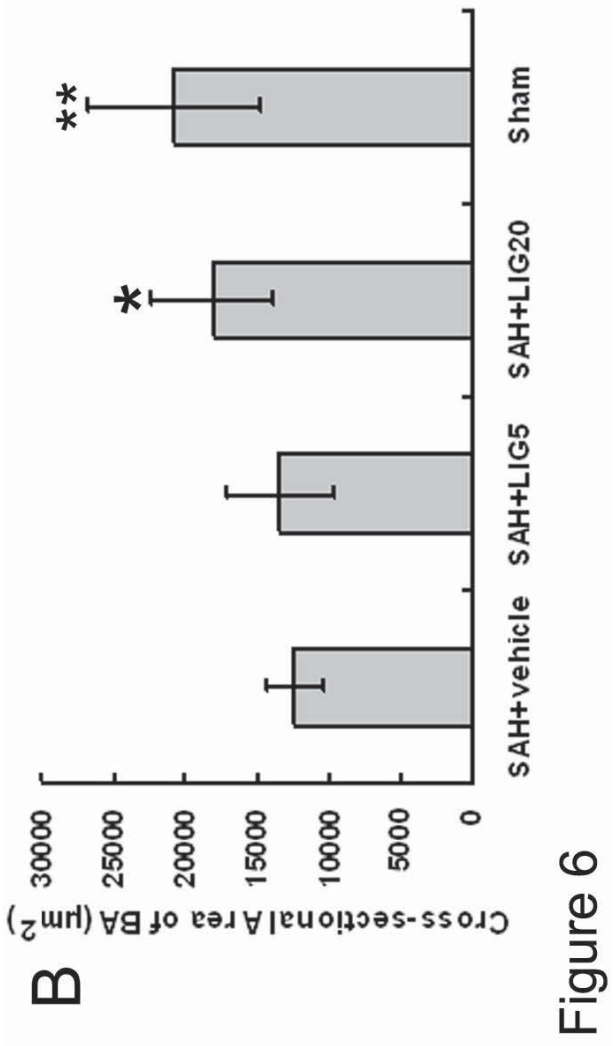

Figure 6

Figure 7

Figure 8

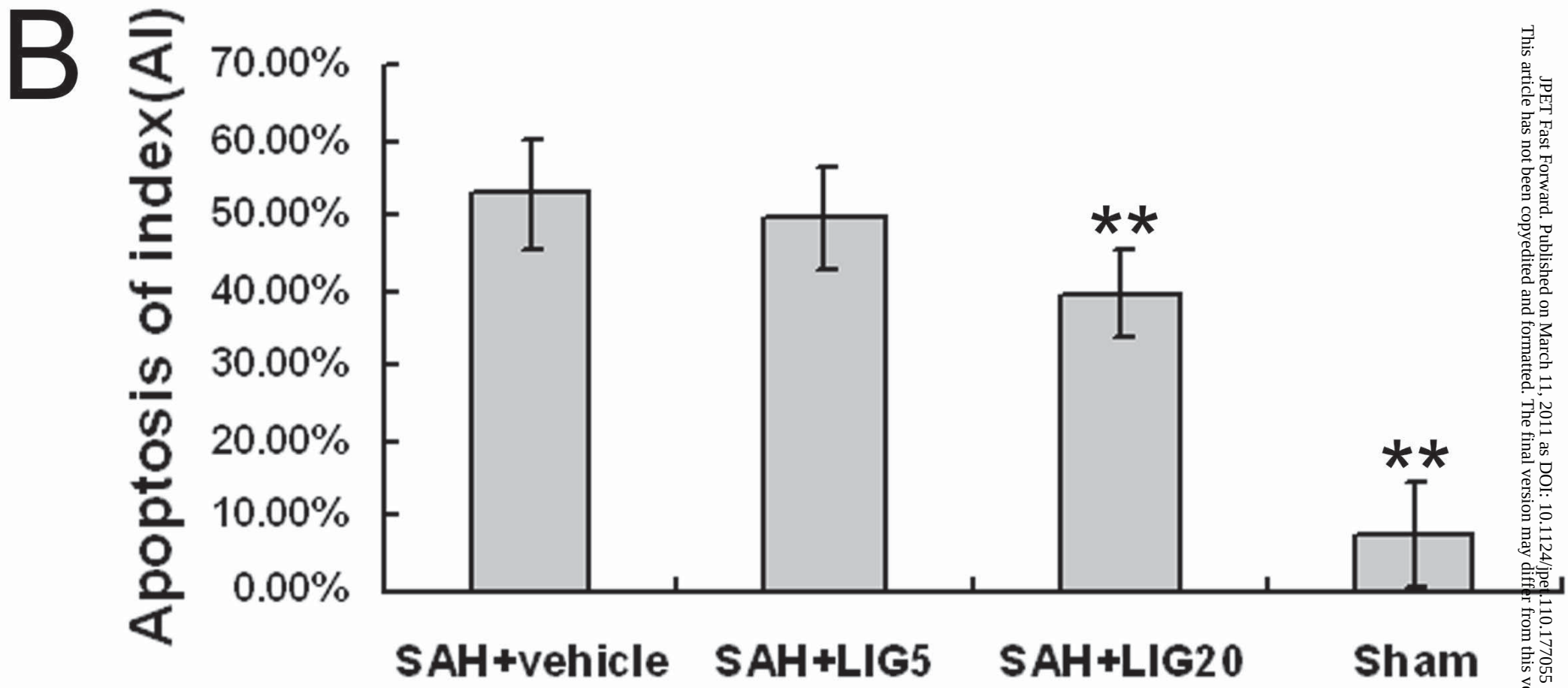

Figure 8

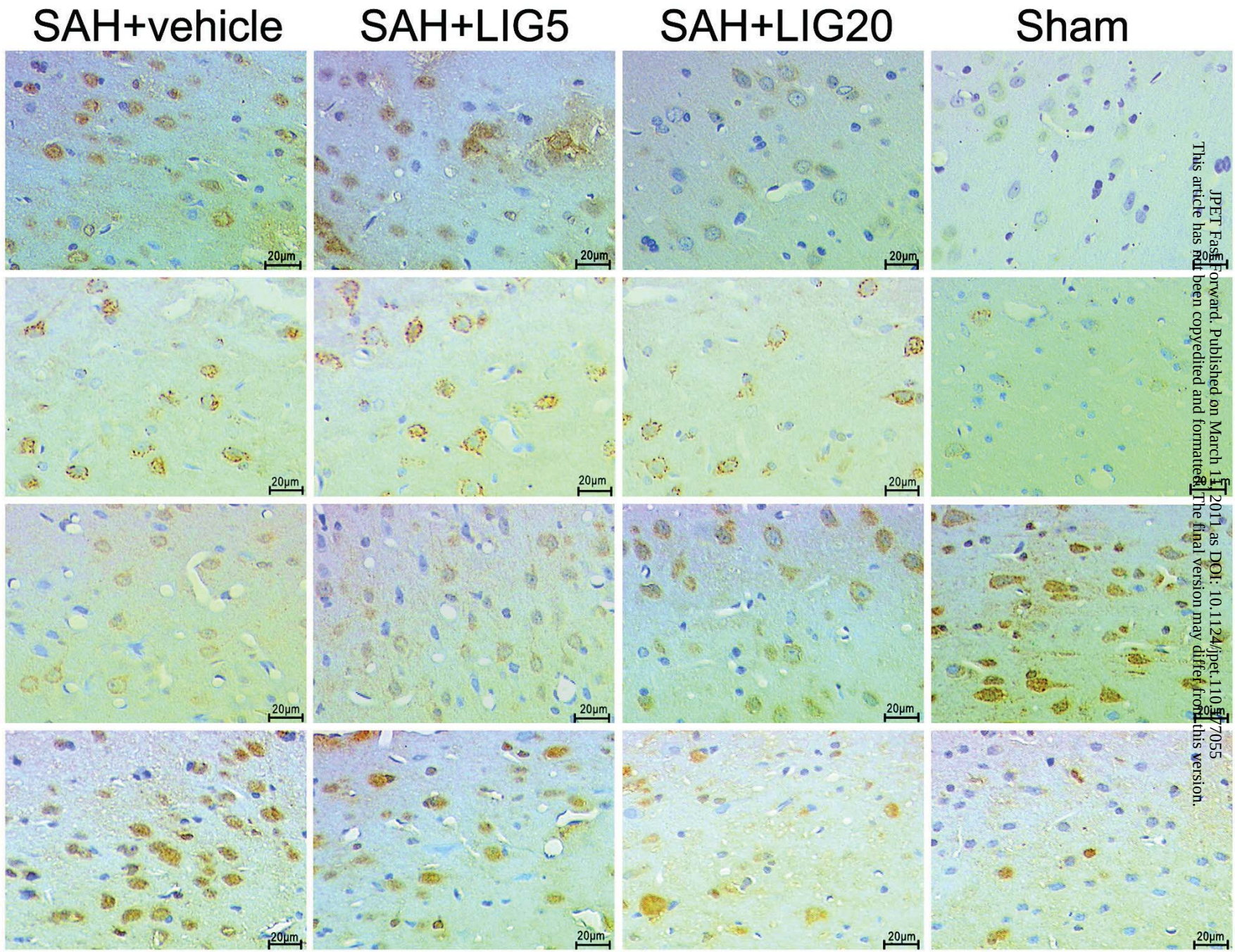

Figure 9

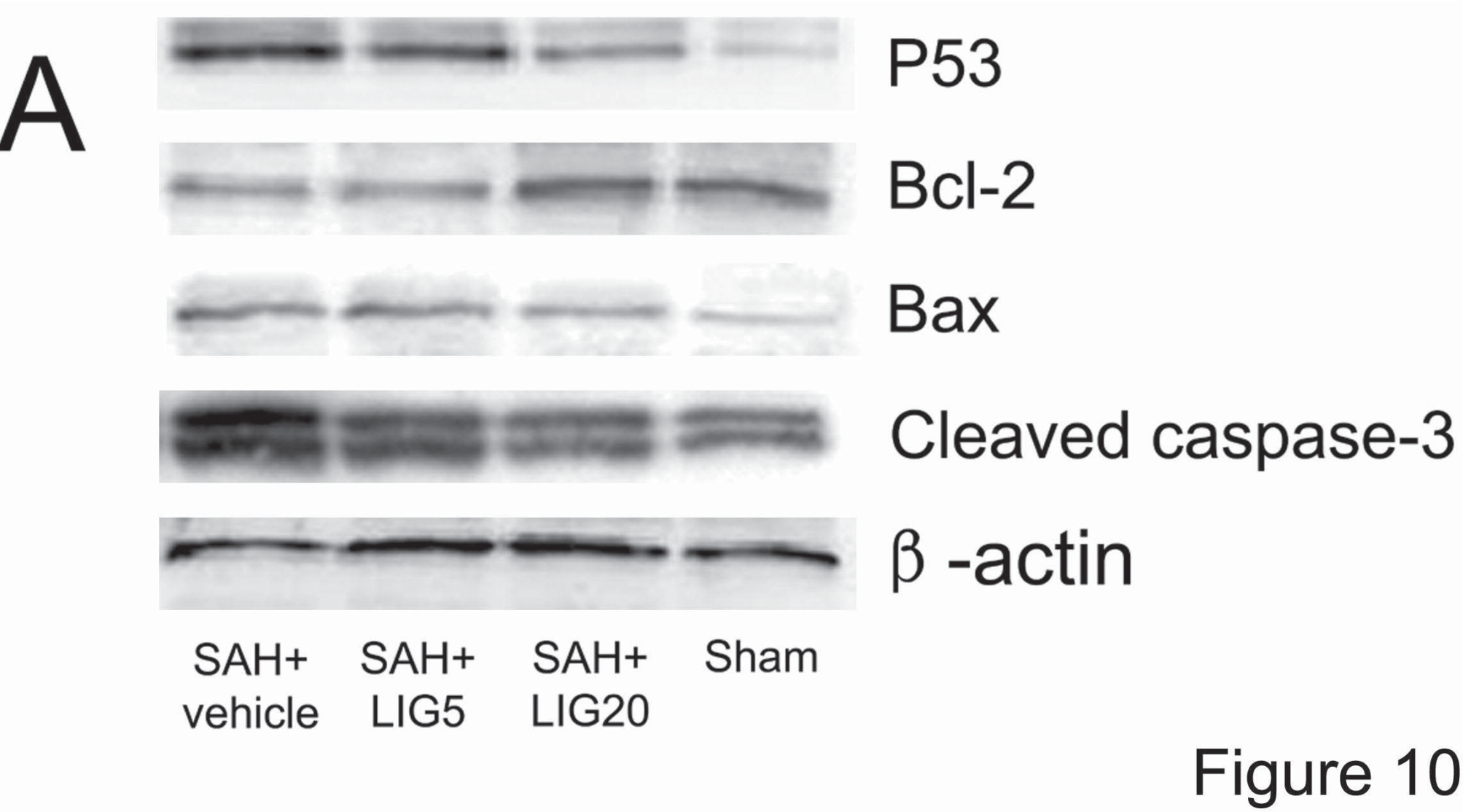

Figure 10

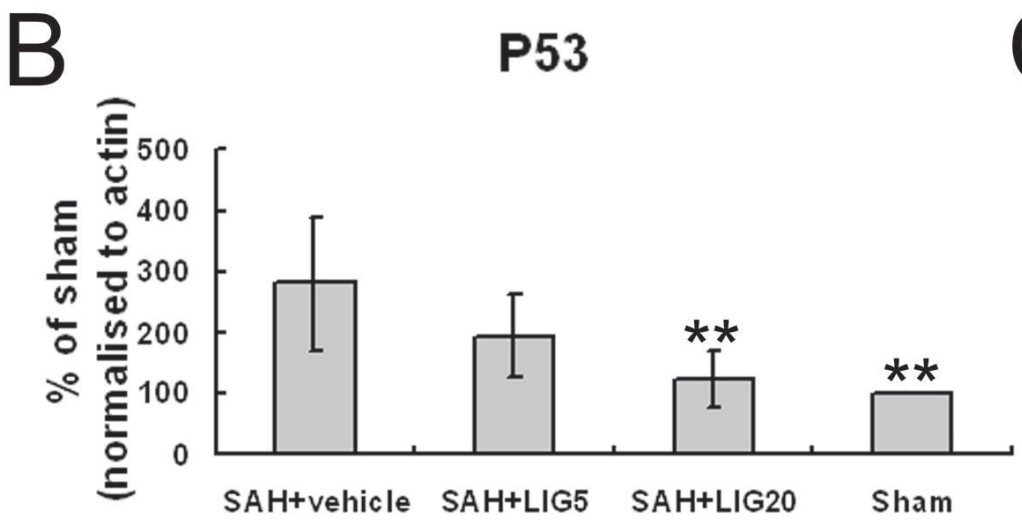

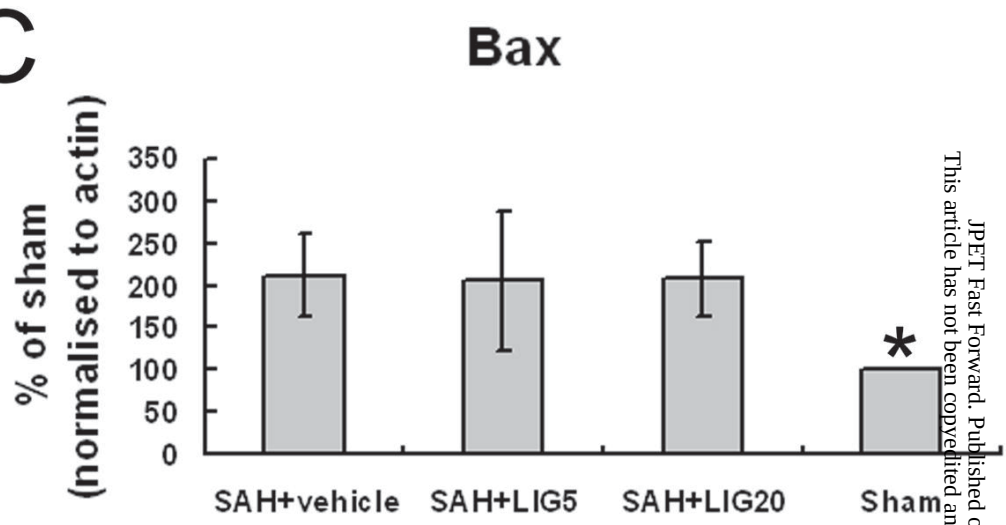

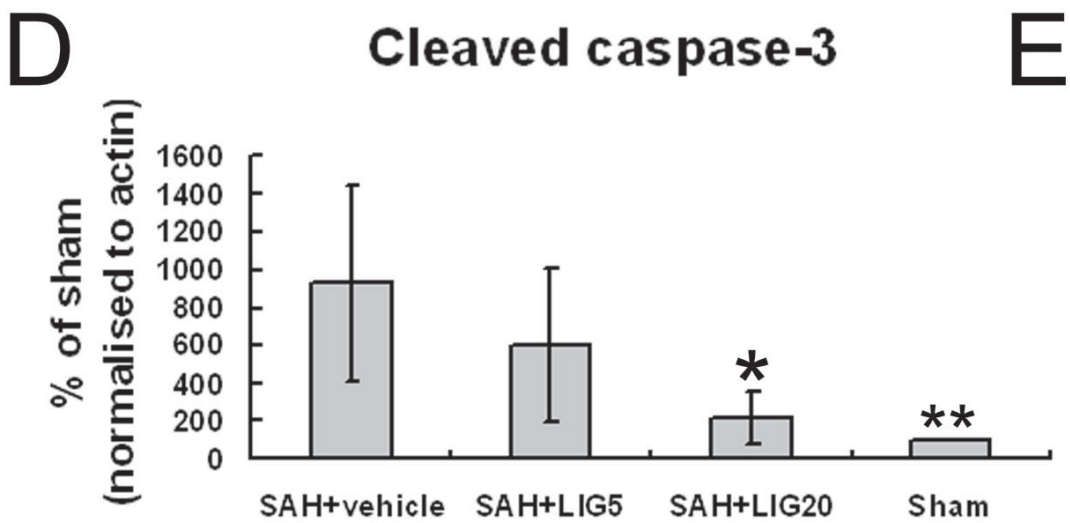

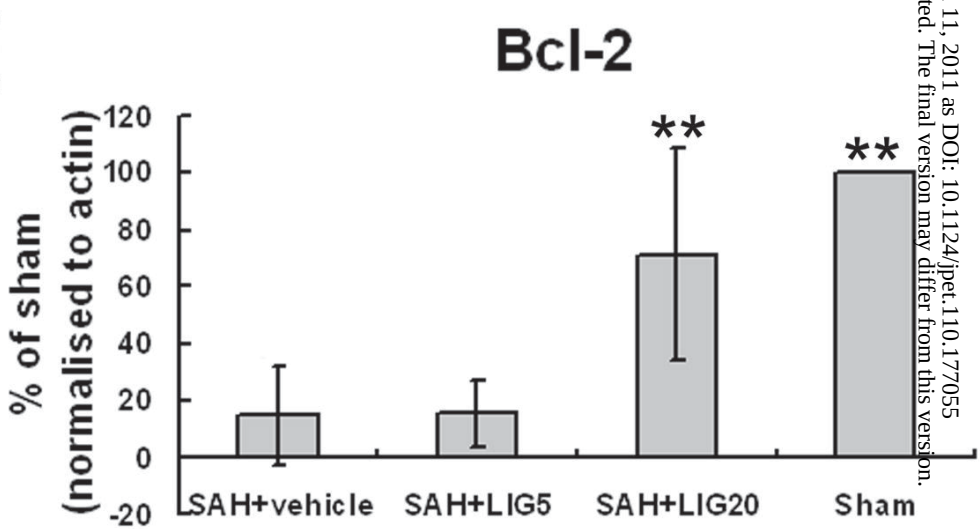

Figure 10